

X-ray diffraction data for graphite to 20 GPa

You Xiang Zhao* and Ian L. Spain

Department of Physics, Colorado State University, Fort Collins, Colorado 80523

(Received 22 September 1987; revised manuscript received 19 December 1988)

X-ray diffraction data have been obtained on polycrystalline graphite at pressures up to 20 GPa. A phase transition is observed at ~ 11 GPa, as evidenced by softening in the interlayer spacing and the observation of new diffraction lines. Below this pressure the variation of the lattice parameters a and c are compared with elastic stiffnesses obtained from ultrasonic measurements. A new value for C_{13} is proposed. The variation $c(P)$ is compared to the recently proposed universal isotherm equation.

INTRODUCTION

Graphite is of considerable experimental and theoretical interest since it is the most highly anisotropic element and is a semimetal. This interest extends to the high-pressure properties of graphite and of its intercalation compounds (see Ref. 1 for a recent review). In spite of this, there is some uncertainty in the compressibilities, which are fundamental to any comparison of experiment and theory (see Ref. 2 for a review).

The crystal structure of graphite is one in which the carbon atoms lie in honeycomb sheets, with extremely strong covalent bonds between the atoms in each sheet. The interlayer bonds are relatively weak, and an $ABAB \dots$ stacking sequence results in hexagonal crystal symmetry, $D6h$.³⁻⁵ An alternative $ABCABC \dots$ stacking sequence (rhombohedral symmetry) is found in defective graphite, always as a mixture with the hexagonal phase.⁶

As a result of the anisotropy of the crystal structure, the compressibility of graphite is highly anisotropic. The planar Young's modulus is 1020 GPa and is higher than for any other substance, while in the c -axis direction it is only 37 GPa at atmospheric pressure (see Ref. 2). There have been several studies of the compressibilities, and the data are not consistent. The results of piston cylinder,⁷⁻⁹ precision elastic constant,¹⁰⁻¹² and x-ray diffraction^{14,15} measurements are reviewed by Kelly.² Representative data from these measurements are shown by him² to 2.5 GPa. It can be seen that the discrepancies between different sets of data are considerable. This is probably due in part to problems with pressure scales used, which have been subject to revision (see Ref. 16, for example).

X-ray diffraction data of Lynch and Drickamer¹⁵ indicated that the hexagonal graphite phase persists to the highest pressure obtained in our study. However, Bundy¹⁶ and Aust and Drickamer¹⁷ reported that the resistivity of certain kinds of graphite increased in such a manner at about 14 GPa that a phase transition was occurring. Aust and Drickamer reported the presence of a cubic phase on release of pressure, but a hexagonal phase was reported by Bundy and Kasper after quenching from about 12 GPa and 2000°C,¹⁸ with diffraction lines recorded in Fig. 1(e). This phase was called hexo-

nal diamond by them. It should be noted that no *in situ* high-pressure x-ray diffraction measurements have been reported on this transition either at room or high temperature.

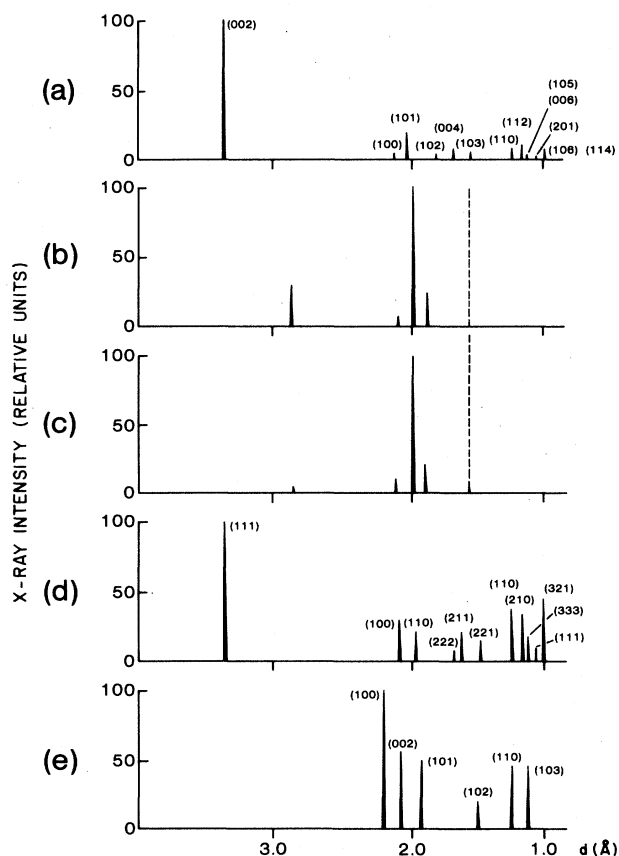


FIG. 1. X-ray diffraction lines for various pressures and comparison with other work: (a) graphite at 0 GPa, (b) pattern obtained at 13.5 GPa, (c) pattern at 16.4 GPa, (d) rhombohedral graphite at 0 GPa, and (e) pattern obtained by Bundy and Kasper at 0 GPa after compression to high pressure. The pattern obtained on release of pressure was an equimixture of (a) and (d). The dashed line represents the window of the diamond-anvil cell.

Most theoretical studies of the compressibilities have used phenomenological models of the interatomic forces.² These models appear to describe the compressional elastic constant C_{33} and its variation with pressure reasonably well to 1 GPa, but are inappropriate for describing the shear modulus C_{44} .¹⁹ More recently, an *ab initio* calculation of the internal energy of graphite at high pressure has been made.²⁰ Such calculations can yield accurate estimates of the compressibilities and high-pressure phases of certain elements.²¹ However, the anisotropy of graphite adds further complexity to the calculations, so that graphite can be looked at as a test case for the theoretical models.

The present work was carried out to obtain accurate data on the crystal parameters of graphite at high pressure using modern pressure scales and improved x-ray diffraction techniques compared to earlier work (see Ref. 22 for a review). This is particularly necessary, since it has been observed in the case of several other elements that earlier data could be significantly improved. In the particular case of the data of Lynch and Drickamer,¹⁵ their pressures are probably overestimated increasingly with higher pressure (see Ref. 22), so that curvature in $a(P)$ data is probably a result of this. These data will be compared with empirical and *ab initio* calculations.

EXPERIMENTAL DETAILS

X-ray diffraction experiments were carried out in a diamond-anvil apparatus using a fixed-anode source and photographic detection using a double-film camera.²³ In order to reduce the error of the d spacings as much as possible, the further film was set 100 mm from the sample, allowing diffraction lines to be observed with $2\theta < 32^\circ$. The standard deviations in c/c_0 and a/a_0 were estimated to be 0.001 and 0.002 Å, respectively. However, the diffraction lines were broadened considerably above the transition, so that the uncertainty in diffraction angles increased by a factor of about 2 or 3, and lattice spacings were uncertain because the crystal structure was not known. Exposure times between 5 and 15 days were required to give reasonable intensity, with the longer exposures being required at higher pressure.

Samples were compressed in 4:1 methanol-ethanol solution, which remains close to hydrostatic to 10 GPa,²⁴ and reasonably hydrostatic to the highest pressure used in our work. Pressure was measured using the ruby-fluorescence scale,²⁵ with a measurement precision of 0.03 GPa below 10 GPa, falling to about 0.2 GPa at 20 GPa due to line broadening in the nonhydrostatic medium. All measurements were carried out at room temperature (295 ± 2 K).

The sample was a fine-grain polycrystalline graphite (Poco ZXF-5Q) (Ref. 26) which was loaded into the sample cavity of diameter 200 μm with a ratio of sample fluid to sample of about 3:1 to ensure that the diamond anvils did not compact the sample directly. This type of material was chosen after experimentation with other types to give a diffraction pattern with reasonably fine grain. (It is to be noted that the process of grinding single-crystal graphite to small crystallite dimensions compared to the

sample cavity diameter of 200 μm produces rhombohedral lines, as noted above.⁶)

Two experiments were carried out on different samples, the first to 12 GPa, at which the diffraction lines became weak, and the second to 20 GPa. This second experiment was carried out on a sample in the form of a disk of thickness 50 μm . When used with diamond anvils of culet diameter 650 μm and a hardened Inconel 718 gasket, this ensured that the diamonds did not touch the sample. In the case of an anisotropic material with weak interplanar bonds such as graphite, this can cause preferential alignment. Even so, the intensity was reduced considerably above 10 GPa. The relatively long exposure times needed for graphite are a result of the low atomic-scattering factor, but the decrease in intensity at high pressure must result from other causes, such as the phase transition discussed in the next section.

EXPERIMENTAL RESULTS

Up to about 12 GPa, three diffraction lines of graphite, indexed as (002), (100), and (101), could be observed within the window afforded by the diamond cell and camera. Their intensities (Fig. 1) were in reasonable agreement with standard compilations,²⁷ except for the (101) line, where our calculations indicate that the ASTM card²⁷ is in error. Experimental data for a/a_0 and c/c_0 are plotted in Fig. 2, and presented in Table I.

At about 10 GPa, the c -axis parameter softened somewhat (Fig. 2), and at 11.8 GPa a steep decrease in c was observed (see note below). After this softening, one extra diffraction line was observed, becoming stronger as pressure was increased, until the pattern with four diffraction lines was observed at 13.5 GPa [Fig. 1(b)]. The relative intensities of the lines continued to change, with the pattern observed at 16.4 GPa being shown in Fig. 1(c). It is noted that the strongest reflection for graphite, the (002), was weakened, and continued to diminish in intensity to the highest pressure. Assuming that this diffraction line

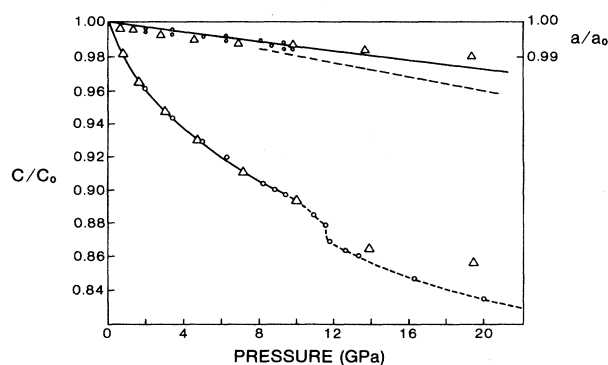


FIG. 2. Present experimental data for the a - and c -axis lattice parameters of graphite to 20 GPa. As explained in the text, the c -axis values above 10 GPa are obtained on the assumption that the line near 3 Å gives the c -axis spacing. The solid line for $a(P)$ is the best fit to the data, the dashed line the prediction using elastic constants from Table I, and the solid triangles the data of Lynch and Drickamer (Ref. 15).

TABLE I. Experimental data for lattice parameters of graphite as a function of pressure.

	<i>P</i> (Gpa)					
	0	2.07	3.5	5.2	6.4	8.2
<i>a</i> (Å)	2.462	2.457	2.455	2.451	2.450	2.448
<i>c</i> (Å)	6.707	6.445	6.324	6.231	6.167	6.060
	8.8	9.5	9.9	11.0	11.6	11.9
<i>a</i> (Å)	2.446	2.445	2.445	2.443	2.442	2.441
<i>c</i> (Å)	6.039	6.022	5.996	5.936	5.892	5.825
	12.7	13.4	16.4	20.0		
<i>a</i> (Å)	2.440	2.439	2.435	2.430		
<i>c</i> (Å)	5.789	5.768	5.764	5.594		

can still be related to the interlayer separation, as for the graphite structure, the decrease in $c(P)$ is plotted in Fig. 2 to 20 GPa. In view of the uncertainty in the structure above about 10 GPa, the a parameter is only plotted to this pressure. If it is assumed that the high-pressure structure is consistent with a mixture of phases, including hexagonal graphite, the values of $a(P)$ deduced from the assumed (100) line lay on a straight line extrapolated from the data shown, but the experimental uncertainty in a was about 0.5%.

DISCUSSION OF RESULTS

The formulas for the volume elastic modulus (bulk modulus) B_v and linear moduli B_a and B_c in terms of the elastic stiffness C_{ij} are

$$B_v = X(C_{11} + C_{12} + 2C_{33} - 4C_{13})^{-1}, \quad (1a)$$

$$B_a = X[2(C_{33} - C_{13})]^{-1}, \quad (1b)$$

$$B_c = X(C_{11} + C_{12} - 2C_{13})^{-1}, \quad (1c)$$

where

$$X = C_{33}(C_{11} + C_{12}) - 2C_{13}^2. \quad (1d)$$

Unfortunately, the error limits in the experimental data (Table II) at $P=1$ atm result in considerably higher un-

certainty in the compressibilities than for typical elements:

$$B_a = 1040 \pm 240 \text{ GPa},$$

$$B_c = 37.0 \pm 1.6 \text{ GPa},$$

$$B_v = 35.8 \pm 1.6 \text{ GPa}.$$

Table II also includes experimental data of the pressure dependence of the elastic constants, evaluated from their slopes at $P=0$. These data allow an estimate to be made of the pressure-lattice-parameter relationships using empirical relationships such as the Murnaghan equation (see Ref. 13 and later in this paper for a discussion). It is noted that experimental values of the pressure dependence of C_{33} , which is crucial for the variation $c(P)$, differ considerably (Table II).

a-axis compression

The compression of the lattice parameter a is less than 1% at 10 GPa, so that a linear fit to the data, with slope equal to the modulus B_a , is appropriate. For instance, using $B_0 = 1580$ GPa and $B'_0 = 5$ with the Murnaghan equation, which should give excellent agreement with data in this limited pressure range ($P/B_0 < 0.013$), the difference in slopes of $a(P)$ calculated using data points

TABLE II. Elastic constants and their pressure derivatives.

Elastic constant	Experimental value ^a (GPa)	Pressure derivative	Second pressure derivative (GPa) ⁻¹
C_{11}	1060±20	39 ^b	
C_{12}	180±20	11 ^b	
C_{13}	15±5	3.1 ^b	
C_{33}	36.5±0.1	9.6 ^b	-1.3±0.6 ^b
		14.7±0.4 ^c	-2.9±1 ^c
C_{44}	4.5±0.05	0.0023	
		5-10 ^c	

^aReference 10.

^bReference 12.

^cReference 11.

at 10 and 20 GPa is less than 1.5%. A second-order fit to the present data, for which $\Delta a/a \approx 0.001$ at 10 GPa and 0.003 at 20 GPa would not be useful. The least-squares fit to the data gives a modulus value of 1580 ± 200 GPa, which is higher than the estimate of 1040 ± 240 GPa based on ultrasonic measurements. The most likely explanation is that the experimental value of C_{13} in Eq.(1b) is incorrect. If the experimental value for $B_a = 1580 \pm 200$ from the present measurements is used together with values of C_{11} and C_{12} from Table I, then the value $C_{13} = 22 \pm 2$ GPa is obtained, which is slightly above the upper error limit of the value obtained by Blakslee *et al.*¹⁰ This contrasts with the negative theoretical estimate for C_{13} obtained by Jansen and Freeman,²⁰ which would give a much lower value of B_a (i.e., ≈ 620 GPa). It is noted that an analysis of the bulk modulus B_a can give a more accurate value for C_{13} than ultrasonic measurements.

The present data can also be compared to covalent-bond models which give the variation of lattice parameters with pressure.²⁸ However, the input data for these models are the elastic constants, and the predicted variation for $a(P)$ is indistinguishable from that of the linear fit to the data because the range of reduced pressure is so small.

c-axis compression

The *c*-axis compression is higher than 10% at 10 GPa, so that equations of state based on the value of C_{33} and its pressure derivative at $P=0$ are inadequate to describe the data. A universal form for the isotherm of solids has been recently proposed.²⁹⁻³¹ It has also been shown³¹ that the limiting forms as V/V_0 approaches zero of several empirical equations are identical with that of the new equation:

$$P(X) = B_0 [3(1-X)/X^2] \exp[\xi(1-X)], \quad (2)$$

where B_0 is the bulk modulus at $P=0$, X is the reduced volume, V/V_0 , and ξ is the pressure derivative of the bulk modulus at $P=0$. Accordingly, a plot of $\ln[P(X)X^2/3(1-X)]$ versus $1-X$ should give a straight line of intercept equal to $\ln B_0$ and slope ξ . Although this equation was derived for isotropic metals, it is instructive to test it with the present data.

Figure 3 plots the experimental data in this form (solid curve). The phase transition is clearly seen, and is similar to curves obtained for other transforming materials.³ The intercept gives a bulk modulus of 30.8 ± 2 GPa, which is significantly less than the accepted value of $B_v = 35.8 \pm 1.6$ GPa derived from elastic constants. As seen from Eq. (1a), this could be due to errors in C_{11} , C_{12} , C_{13} , and C_{33} or to the inapplicability of Eq. (2) to an anisotropic material. The results discussed below suggest that the accepted value of C_{33} is reasonable. Since B_v does not depend strongly on C_{13} , whose value has been fixed from B_a , and the parameters C_{11} or C_{12} are known accurately from ultrasonic data (Table I), the present data point to a limitation in the applicability of Eq. (2).

The data are plotted in an alternative form in Fig. 3,

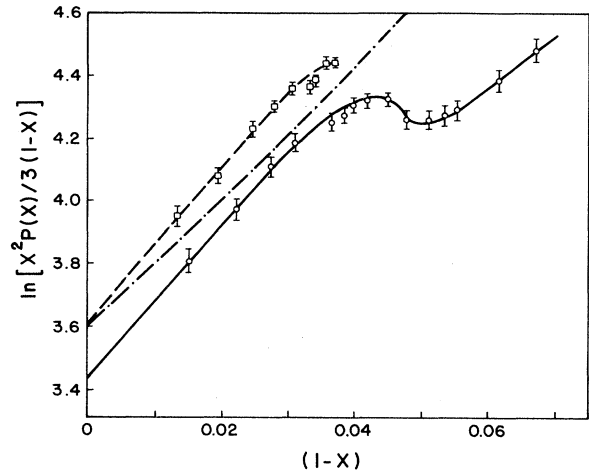


FIG. 3. Plot of $\ln[X^2 P(X)/3(1-X)]$ vs $1-X$ (the units of P are GPa). The open circles are for $X^3 = V/V_0$, fitted with the solid line, the squares are for $X^3 = C/C_0$, fitted with a dashed line, and the dotted-dashed line is for the Lennard-Jones equation (3), with $C_{33} = 36.5$ GPa.

where X is replaced by $X' = c/c_0$ with a dashed line. In this case the relatively unimportant contribution from in-plane contraction is neglected. The intercept equals the acoustic value of $B_c = 37$ GPa within experimental error, but the initial slope (25 ± 3) is much higher than either of the previous determinations from velocity measurements (see Table I). This is consistent with fitting $P(c/c_0)$ data in Fig. 2 to empirical equations, in which it is found that the ultrasonic data of Ref. 12, with a higher value of C'_{33} , give c/c_0 values which fit the data more nearly than using values from Ref. 11. The discrepancy between the $P(c/c_0)$ values using data from Ref. 12 and the experimental data is in the direction that a higher value of C'_{33} is called for.

A Lennard-Jones interplanar potential model is often used for graphite, giving good agreement with thermal and elastic data.³² The resulting isotherm equation, assuming negligible *a*-axis contraction, is²

$$P = \frac{C_{33}}{6} \left[\left(\frac{c_0}{c} \right)^4 - \left(\frac{c_0}{c} \right)^{10} \right]. \quad (3)$$

This equation is plotted in Fig. 3 as the dotted-dashed line, using $B_c = C_{33} = 36.5$ GPa. It can be seen that the line is straight at low compressions, but bows upwards at higher values, consistent with the pressure derivative C'_{33} increasing with pressure. The initial slope is 19.7, which is considerably larger than either of the values estimated from elastic data (Table I), but lower than that required to fit the present data.

Phase transition at high pressure

Both the softening of the interlayer forces near 12 GPa (Figs. 1 and 2) and changes in the diffraction pattern [Figs. 1(b) and 1(c)] argue for a phase transition near this pressure. It was not possible to assign a structure to the

high-pressure phase, but it was possible to rule out the possibility of its being hexagonal diamond,¹⁸ particularly since this phase was not obtained on release of pressure, but an approximately equivolume mixture of hexagonal and rhombohedral graphite. It is possible that the phase transition is related to that observed in resistivity measurements^{16,17} if allowance is made for differences in pressure scales.²² Unfortunately, shock data have been aimed at a higher pressure and temperature range. Recent measurements³³ of higher precision still show considerable scatter at pressures between 10 and 20 GPa, so that a transition such as that observed here cannot be confirmed from these data.

The question of the origin of the softening can only be answered by obtaining data on higher-index peaks. This can be obtained, in principle, by using synchrotron radiation. An experiment on a single crystal of graphite in a compressing medium such as argon using synchrotron radiation is recommended. Such measurements would also be invaluable for increasing the precision of measurement of $a(P)$, and of determining a precise value of C_{13} .

CONCLUSIONS

X-ray diffraction data have been obtained on polycrystalline graphite to 20 GPa, from which it was deduced that a phase transition occurred at ~ 11 GPa, which ac-

counts for a discontinuity found in previous resistivity measurements. A mixture of hexagonal and rhombohedral graphite was found on release of pressure, so that the high-pressure phase was probably planar, and not related to the formation of three-dimensional bonds, as found in metastable phases at higher pressure and temperature. It was not possible to specify the high-pressure phase from the limited data available.

The data to about 10 GPa were analyzed to give $a(P)$ and $c(P)$. These data were then analyzed in terms of a function proposed as a universal isotherm. It was found that the in-plane modulus B_a was higher than the value based on elastic stiffnesses, and allowed a new value of C_{13} to be proposed.

ACKNOWLEDGMENTS

Thanks are due to the U.S. Air Force Office of Scientific Research for (Contract No. F49620-84-K-006) supporting this work. The assistance of Carmen Rocca, Charles Bowers, and Donald Trock is gratefully acknowledged. Thanks are also due to Henri Jansen for providing a copy of his work prior to publication and for pointing out an error in our analysis of C_{13} , and to Dr. John Shaner for communicating results of his work prior to publication.

*On leave from Institute of Physics, Chinese Academy of Science, Beijing, China.

¹R. Clarke and C. Uher, *Adv. Phys.* **33**, 469 (1984).

²B. T. Kelly, *The Physics of Graphite* (Applied Science Publishers, London, 1981).

³A. W. Hull, *Phys. Rev.* **10**, 661 (1917).

⁴J. D. Bernal, *Proc. Phys. Soc. London, Sect. A* **106**, 749 (1924).

⁵O. Hassel and H. Mark, *Z. Phys.* **18**, 291 (1924).

⁶H. Lipson and A. R. Stokes, *Proc. Phys. Soc. London, Sect. A* **181**, 101 (1942).

⁷T. W. Richards, *J. Am. Chem. Soc.* **1934** (1915).

⁸J. Basset, *Compt. Rend.* **213**, 829 (1941).

⁹P. W. Bridgman, *Proc. Am. Acad. Arts Sci.* **76**, 9 (1945); **76**, 55 (1945).

¹⁰O. L. Blakslee, D. G. Proctor, E. J. Seldin, G. B. Spence, and T. Weng, *J. Appl. Phys.* **41**, 3373 (1970).

¹¹J. F. Green, P. Bolsaitis, and I. L. Spain, *J. Phys. Chem. Solids* **34**, 1927 (1973).

¹²W. B. Gauster and I. J. Fritz, *J. Appl. Phys.* **45**, 3309 (1974).

¹³L. Knopff, in *High Pressure Physics and Chemistry*, edited by R. S. Bradley (Wiley, New York, 1951), p. 227.

¹⁴S. S. Kabalkina and L. F. Vereschagin, *Dokl. Akad. Nauk SSSR* **131**, 300 (1960) [*Sov. Phys.—Dokl.* **5**, 373 (1960)].

¹⁵R. W. Lynch and H. G. Drickamer, *J. Chem. Phys.* **44**, 181 (1966).

¹⁶F. P. Bundy, *J. Chem. Phys.* **38**, 631 (1963).

¹⁷R. B. Aust and H. G. Drickamer, *Science* **140**, 817 (1963).

¹⁸F. P. Bundy and J. S. Kasper, *J. Chem. Phys.* **46**, 3437 (1967).

¹⁹J. F. Green and I. L. Spain, *Phys. Rev. B* **11**, 3935 (1975).

²⁰H. J. F. Jansen and A. J. Freeman, *Phys. Rev. B* **35**, 8207 (1987).

²¹M. L. Cohen, *Science* **234**, 549 (1986).

²²A. Jayaraman, *Rev. Mod. Phys.* **55**, 65 (1983).

²³I. L. Spain, D. R. Black, Z. L. D. Merkle, J. Z. Hu, and C. S. Menoni, *High Temp. High Pressures* **16**, 507 (1985), and references therein.

²⁴G. J. Piermarini, S. Block, and J. S. Barnett, *J. Appl. Phys.* **44**, 5377 (1973).

²⁵J. D. Barnett, S. Block, and G. J. Piermarini, *Rev. Sci. Instrum.* **44**, 1 (1973).

²⁶Poco Graphite Inc., Dekatur, TX 76243, Type ZXF-5Q.

²⁷American Society for Testing Materials, Philadelphia, PA, Crystallographic Data, Card 12-212.

²⁸V. N. Zharkov and V. A. Kalinin, *Equations of State for Solids at High Pressures and Temperatures* (Consultants Bureau, New York, 1970).

²⁹P. Vinet, J. Ferrante, J. R. Smith, and J. H. Rose, *J. Phys. C* **19**, L467 (1986).

³⁰P. Vinet, J. Ferrante, J. H. Rose, and J. R. Smith, *J. Geophys. Res.* **92**, 9319 (1987).

³¹H. Schlosser and J. Ferrante, *Phys. Rev. B* **37**, 4351 (1988).

³²B. T. Kelly and P. L. Walker, *Carbon* **8**, 211 (1970).

³³J. Shaner (unpublished data), of Los Alamos Scientific Laboratory, communicated privately.